Mouse model of Alzheimer's Disease Demonstrates Differential Effects of Early Disease Pathology on Various Brain Regions.

Liting Deng[1], Vivek K. Gupta[2#], Yunqi Wu[1], Kanishka Pushpitha[2], Nitin Chitranshi[2], Veer B Gupta[3], Matthew J. Fitzhenry[4], Masoud Zabet Moghaddam[5], Tim Karl[6], Ghasem Hosseini Salekdeh[1], Stuart L. Graham[2], Paul A. Haynes[1], Mehdi Mirzaei[2#]

[1]Department of Molecular Sciences, Faculty of Science and Engineering, Macquarie University, Sydney, NSW, Australia

[2]Faculty of Medicine and Health and Human Sciences, Macquarie University, Sydney, NSW, Australia

[3] School of Medicine, Deakin University, Geelong, VIC, Australia

[4]Australian Proteome Analysis Facility (APAF), Macquarie University, Sydney, NSW, Australia

[5]Center for Biotechnology and Genomics, Texas Tech University, Lubbock, TX, United States

[6]School of Medicine, Western Sydney University, Penrith, NSW, Australia

Corresponding authors

Mehdi Mirzaei – mehdi.mirzaei@mq.edu.au

Faculty of Medicine and Health and Human Sciences, Macquarie University, Sydney, NSW, Australia

Vivek K Gupta – vivek.gupta@mq.edu.au

Faculty of Medicine and Health and Human Sciences, Macquarie University, Sydney, NSW, Australia

Received: August 01, 2020; Revised: January 31, 2021; Accepted: February 01, 2021

This article has been accepted for publication and undergone full peer review but has not been through the copyediting, typesetting, pagination and proofreading process, which may lead to differences between this version and the Version of Record. Please cite this article as doi: 10.1002/pmic.202000213.

Abstract: Different parts of the brain are affected distinctively in various stages of the Alzheimer's disease (AD) pathogenesis. Identifying the biochemical changes in specific brain regions is key to comprehend the neuropathological mechanisms in early pre-symptomatic phases of AD. Quantitative proteomics profiling of four distinct areas of the brain of young APP/PS1 mouse model of AD was performed followed by biochemical pathway enrichment analysis. Findings revealed fundamental compositional and functional shifts even in the early stages of the disease. This novel study highlights unique proteome and biochemical pathway alterations in specific regions of the brain that underlie the early stages of AD pathology and will provide a framework for future longitudinal studies. The proteomic data were deposited into the ProteomeXchange Consortium via PRIDE with the identifier PXD019192, username reviewer39421@ebi.ac.uk, and password olHioahM, respectively.

Key words

Alzheimer's disease, proteomics, amyloid beta, hippocampus, cortex, cerebellum, APP/PS1

Alzheimer's disease (AD) is a chronic ageing related neurodegenerative disease which is characterized by loss of neurons and synaptic connections in the vulnerable regions of the brain including the hippocampus and cerebral cortex[1]. The disease is characterized by perturbations in amyloid β and tau protein expression in the brain [2, 3]. Accumulation of amyloid β fibrillar assemblies and extracellular plaques is a hallmark representation of AD pathology. APP/PS1 is a transgenic mouse model of AD that expresses human mutant amyloid precursor protein (APP) and presenilin 1 (PSEN1) genes and has been extensively used in AD research [4]. The disease progressively affects memory formation and its retrieval processes in the brain which gradually extends to visuospatial, language, attention, logic, and executive function deficits [5]. An insidious characteristic of the disease is that various brain regions are differently affected during the course of the disease [6-9].

The pathophysiological process of AD begins with a long "preclinical" phase many years before the disease is diagnosed. Substantial molecular and neurodegenerative changes occur in the initial stage of AD even before the cognitive symptoms are evident, which makes the early diagnosis of AD vital and key to any timely disease stabilization and treatment [10]. Earlier discovery of AD associated cellular response and molecular changes will improve therapeutic strategies, such as medication or life-style changes, to potentially reduce the disease progression [11]. However,

diagnosing AD in the initial stage is difficult and lacks accuracy since the early events in the onset of the pathology are yet to be fully elucidated.

The neuropathology is believed to begin initially in the hippocampus and entero-rhinal cortical regions which gradually encompasses frontal, parietal, and temporal regions of the brain [12]. However, despite extensive research effort and progress in the field, molecular mechanisms of disease onset and the sequence of events in the brain that underly initial stages of AD pathology remain ill-defined. In this study, we aimed to identify the molecular changes that occur in different regions of the brain during early stages of AD pathology viz. hippocampus, frontal and parietal cortices, and cerebellum. These changes were studied in young APP/PS1 mice brain regions using comparative TMT-labelled quantitative proteomics [2]. APP/PS1 mice show progressive brain pathology with animals exhibiting memory insufficiencies by 3 months of age with initial evidence of amyloid deposition in hippocampus and cerebral cortical regions. The animals start exhibiting various features of loss of social interaction, and hippocampal and cortical atrophy accompanied by neuronal loss between 6-12 months of age [13]. Therefore, we selected 2.5-month-old APP/PS1 mice, by which age, amyloid accumulation has initiated but without an element of neuronal cell death in the brain, that would confound our ability to study the initial molecular changes.

Four different regions of APP/PS1 and WT mice (n=5 each) brains were surgically excised based on published geometrical co-ordinates [14]. Hippocampus and cortex are predominantly affected in AD while cerebellum is largely spared in the initial stages of the disease [6]. Proteins were extracted from each brain tissue with ice-cold lysis buffer (50 mM Tris-HCl, pH7.5, 150 mM NaCl, 1% NP40, 1 mM EDTA, 0.1% SDS, protease inhibitor cocktail (ThermoFisher) using probe sonicator [15]. Extracted proteins were subjected to reduction, alkylation followed by digestion before TMT labeling as described previously [16]. 45 µg of peptides per sample were subjected to the labeling using 10-plex TMT reagents (Thermo Fisher). Four independent 10-plex TMT experiments were performed to accommodate a total of 40 biological samples (10 samples per TMT experiment/per brain area, 5 APP/PS1 and 5 WT). The complete sample processing workflow and TMT labeling strategy is presented in the Fig. S1. Dried TMT labelled peptides from each fraction were dissolved in 20 µL of 0.1% formic acid and analyzed on a Q Exactive Orbitrap mass spectrometer coupled to an EASY-nLC1000 nanoflow HPLC system (Thermo Scientific, USA). The MS raw data files were processed in Proteome Discoverer V2.1 (Thermo Scientific, USA) using search engine Mascot (Matrix Science, UK). Percolator algorithm was used to discriminate correct from incorrect peptide-spectrum matches, and calculate statistics including q-value (FDR) and posterior error probabilities. Relative quantitation of proteins was achieved by pairwise comparison of TMT reporter ion signal to noise (S/N) ratios. Proteins from Proteome Discoverer were further analyzed using the in house TMTPrepPro analysis pipeline [17]. Relative quantitation of protein abundance in specific brain tissue with AD compared to

control was derived from the ratio of the TMT label S/N detected in each brain tissue and differentially expressed proteins between AD and control were identified based on student *t*-tests. Differential expression required the proteins to meet both fold change ≥1.20 (up-regulated) or <0.833 (down-regulated)], and p-value cut-off ≤ 0.05 [18]. Cytoscape with String as plugin was used to classify regulated proteins in different brain areas according to their enriched biological processes and pathways.

Mass spectrometry analysis identified 4758, 5045, 4781 and 5225 proteins (1% FDR) from four independent TMT-labelled experiments carried out respectively on the hippocampus, cerebellum, parietal and frontal cortex regions of young APP/PS1 mice (Table S1). Although, about 5000 proteins were identified in all regions; the proteome response across regions was greatly varied (Fig. 1). As expected, the highest proteome perturbation was detected in the hippocampus (1321 differentially modulated proteins) and frontal cortex (1331 proteins with significant regulation;≥ 1.2- or ≤ 0.833-fold change, p value ≤ 0.05). This is in contrast to only 155 proteins that demonstrated an altered abundance in the cerebellum tissue. These results corroborate previous reports that cerebellum is relatively less affected in AD pathology. Of note, APP peptides were identified in all the regions of the brain and showed an increased abundance. These peptides may either be derived from APP holoprotein or 37-49 amino acid residue Aβ assemblies following the cleavage of parent protein. Hierarchical clustering analysis of differentially expressed proteins for each specific brain regions (Fig. 1A-D) illustrated overall consistency between biological replicates in both APP/PS1 and WT animals. While 25% of the proteins identified in the hippocampus and frontal cortex regions were significantly affected in APP/PS1 mice, only 3% and 16% of protein respectively were changed in the cerebellum and parietal cortex regions. This data indicated that these regions were relatively less impacted during early disease stages. There were 739, 95, 333 and 649 proteins with increased expression in the hippocampus, cerebellum, parietal and frontal cortex regions respectively in the APP/PS1 animals (Fig. 1E-I), while 582, 60, 445 and 682 proteins were decreased in expression in those tissues in APP/PS1 mice listed above. Although, the number of differentially expressed proteins was comparable between hippocampus and frontal cortex, a significant proportion of the differentially expressed proteins identified in hippocampus were oppositely regulated in the two cortical regions. The overlap of differentially expressed protein across four different brain regions is represented using the Venn diagram plot (Fig. 1J) indicating that only 14 proteins that were altered in the cerebellum were also differentially affected in the other three brain regions. In comparison, there was an overlap of 234 proteins, that were differentially modulated in abundance between hippocampus and two cortical areas. Further analysis revealed that while 393 proteins were identified as commonly affected between the two cortices, 367 proteins were identified amid hippocampus and parietal cortex and 491 proteins within hippocampus and frontal cortex regions (Fig. 1J; S2).

Hippocampus is the key part which is reported as one of the earliest and most severely affected areas of brain AD and due to its central role in memory processing [19]. The differentially expressed proteins were analyzed and classified based on their pathway enrichment and functional protein network using string software. The analysis was performed aiming to identify molecular mechanisms and biological processes underlying AD pathophysiology in young APP/PS1 mice. The interactions among proteins and associated pathways are demonstrated in Fig. 2. The analysis aimed to elucidate crucial biochemical networks and biological processes that are affected in the hippocampus of young AD animals. A series of AD associated markers were enriched in the hippocampus that comprised pathways associated with Alzheimer's disease, oxidative phosphorylation, glutamatergic synapse, GABAergic synapse, retrograde endocannabinoid signaling, long-term potentiation, and calcium signaling modules. Comparingly, the expression of same proteins and pathways was negatively regulated in frontal and parietal cortex regions. Excitatory glutamate and inhibitory gamma-aminobutyric acid (GABA) neurotransmitters work together to control the overall level of excitation in the brain. Retrograde messengers adjust the precise timing of neurotransmitter released from the pre-synapse, thus modulating synaptic efficacy and neuronal activity [20]. A balanced interaction is required to maintain the physiological homeostasis, while prolonged imbalance can lead to nerve damage and other associated underlying pathological conditions. Similar observations have been reported previously where proteins linked to inflammatory and neuronal homeostasis were shown to exhibit correlation with human AD neuropathology[8]. Another comprehensive gene expression study in AD animal models revealed positive correlation of immune system and synaptic changes with amyloid beta with disease progression[7]. Intracellular Ca^{2+} signaling is closely associated with the retrograde endocannabinoid signaling and neuronal function. The formation and storage of memories depend on brief high concentration spikes of Ca^{2+} that activate and enhance the process of long-term potentiation [21] (Fig. 2, S4, S5). In contrast, a negative regulation of proteins was detected in other crucial networks including myelination, neurofilament cytoskeleton organization, spliceosome and glutathione metabolism networks that encompassed the proteins that were downregulated in abundance indicating that these pathways were negatively affected in AD. Interestingly, these down regulated proteins were elevated in both the cortex areas and remained unaltered in the cerebellum. The results obtained from this research highlight important information on brain-region specific protein expression changes occurring in the early stages of AD. Spliceosome is crucial for pre-mRNA splicing and the production of mature RNA [22]. We identified 14 down regulated hippocampal proteins associated with RNA splicing or mRNA processing. Eight of these proteins were recognized as the cellular components of the spliceosome complex among which Prpf4, Prpf40a, Snrnp70 and Rbm22 were classified as elements of the specific U2-type spliceosome which mainly catalyzes the removal of U2-type introns. Further, eight down regulated proteins enriched in glutathione metabolism pathway with four of them being glutathione S-transferase (GST)

enzymes, which catalyze conjugation of reduced glutathione to a wide range of substrates, usually resulting in detoxification. 17 down regulated proteins in hippocampus were associated with myelination, and most of these proteins were up regulated in both the cortices. There were almost no changes in the cerebellum region. Amongst these, 12 proteins comprised integral components of the myelin sheath of neurons (Fig. S6, S7).

From the hippocampus data we identified 27 proteins with increased abundance which were classified as related to the Alzheimer's disease process in the KEGG pathway. KEGG analysis, provides insights into the broad functional relevance of the differentially affected proteins. A unique feature of this evaluation was that although these proteins were altered in hippocampus, these were not significantly modulated in other three regions of the brain (Fig. 3A, 3B). APP which is an archetypal protein associated with AD pathology was an exception and elevated across all the areas. The greatest increase for APP was however observed in the hippocampus while the frontal cortex region demonstrated relatively a lesser amount of upregulation. The APP expression was validated in immunoblotting using APP specific antibodies, with actin as loading control (Fig. 3C and 3D). Likewise, Nicastrin (Ncstn) which is a crucial constituent of gamma secretase complex that is involved in APP processing and generation of Aβ peptides, was up regulated in all the brain regions expect for the frontal cortex, where it was not altered [23].

Accumulating evidence from human and animal studies suggests early molecular defects in oxidative phosphorylation (OXPHOS) leading to mitochondrial dysfunction in AD [24]. OXPHOS, which accomplishes the ATP production following protons re-entering the mitochondria, was severely impacted in APP/PS1 mice with 23 proteins that were enriched in the hippocampus (Fig. 3B). Remarkably, OXPHOS analysis revealed that 12 proteins that classified under AD umbrella in hippocampus, were also integral to the OXPHOS network. Amongst these, 16 proteins were recognized as components of the inner mitochondrial membrane protein complex which is mainly involved in regulating the oxido-reductase machinery. Mitochondrial OXPHOS system comprises five key enzyme complexes from complex I to V involving 80 proteins [25]. Out of the AD associated proteins from the hippocampus region, seven were identified to be part of the mitochondrial respiratory chain complex I (mt-Nd1, mt-Nd3, mt-Nd4, mt-Nd5, Ndufa9, Ndufb4 and Ndufs7), two (Uqcrq and Uqcr11) as belonging to the ubiquinol-cytochrome c reductase complex (Complex III), and four as subunits of the respiratory chain complex IV (mt-Co1, mt-Co2, mt-Co3 and Ndufa4) (Fig. S3). 10 proteins also constituted various components of the ATPase/ATP synthase, Complex V, which is placed in the inner membrane of mitochondria and serves as the powerhouse of the cell by synthesizing ATP. Of note, a large proportion of hippocampal OXPHOS regulated proteins were not significantly affected in the frontal and parietal cortexes of APP/PS1 mice. Parallel to the OXPHOS findings, we observed that glutamatergic and GABAergic synapse and retrograde endocannabinoid

signaling pathways were enhanced in hippocampus while these networks exhibited a reverse association in frontal and temporal cortex regions with significant downregulation of these proteins. Cerebellum proteome for these pathways remained relatively unaltered (Fig. S4). For the spliceosome, glutathione metabolism and neurofilament cytoskeleton networks, while the hippocampus proteins were downregulated in abundance, parietal cortex demonstrated an increase in several components associated with these networks and processes (Fig. S6). Further, a similar trend of downregulation of several myelination pathway associated proteins was also detected for hippocampus region which again showed a reverse relationship with the abundance of these proteins in the frontal and parietal regions (Fig. S7).

In conclusion, this data set reflects the proteomics alterations in four different regions of the brain and provides molecular insights into the early changes that might be associated with early brain pathology in APP/PS1 mice. The results elucidate how different regions of the brain are affected during initial stages of the disease process before more wide-spread cellular loss and functional deficits ensue as the disease progresses. A significant finding is that hippocampus and cortex areas are the regions which experience the highest impact during early stages of the disease compared to the cerebellum, which is commonly known as the non-vulnerable area of the brain in AD. The impact was primarily assessed based on the number of differentially modulated proteins as well as pathways modulated in each area. Intriguingly, several biochemical networks show opposing modulation in the hippocampus and two cortex regions. The exact molecular basis of these opposing action is not clear. However, these may indicate differential effects of amyloid toxicity in the tissues or a differential response to counter the amyloid build-up. It has been shown in APP/PS1 mice, that amyloid plaque formation starts at approximately six weeks of age in the neocortex while deposits appear in the hippocampus at about three to four months. Therefore, the differential effects observed in hippocampus and cortex may be attributed to region specific compensatory responses to amyloid beta, despite the fact that APP was observed to be upregulated in all four studied regions of the mouse brain[26]. Alternatively, it is possible that two brain regions are at different stages of the disease process and the biochemical changes will eventually converge to show a similar pattern of molecular neuropathological changes. Nevertheless, this data will serve as important reference material for future studies investigating early AD changes in different regions of the brain. Longitudinal studies that follow up the animals at different age groups will delineate the progressive region-specific changes in AD.

Acknowledgements: We acknowledge support from National Health and Medical Research Council (NHMRC) Australia, Hilcrest foundation and Macquarie University.

[1] Y. Vyas, J. M. Montgomery, J. E. Cheyne, Front Neurosci 2020, 14, 266.

[2] M. Mirzaei, K. Pushpitha, L. Deng, N. Chitranshi, V. Gupta, R. Rajput, A. B. Mangani, Y. Dheer, A. Godinez, M. J. McKay, K. Kamath, D. Pascovici, J. X. Wu, G. H. Salekdeh, T. Karl, P. A. Haynes, S. L. Graham, V. K. Gupta, Mol Neurobiol 2019, 56, 6017.

[3] V. B. Gupta, V. K. Gupta, R. Martins, N Engl J Med 2013, 369, 1660; V. B. Gupta, N. Chitranshi, J. den Haan, M. Mirzaei, Y. You, J. K. Lim, D. Basavarajappa, A. Godinez, S. Di Angelantonio, P. Sachdev, G. H. Salekdeh, F. Bouwman, S. Graham, V. Gupta, Prog Retin Eye Res 2020, 100899.

[4] V. K. Gupta, N. Chitranshi, V. B. Gupta, M. Golzan, Y. Dheer, R. V. Wall, D. Georgevsky, A. E. King, J. C. Vickers, R. Chung, S. Graham, Neurosci Lett 2016, 623, 52.

[5] S. Karantzoulis, J. E. Galvin, Expert Rev Neurother 2011, 11, 1579.

[6] J. Xu, S. Patassini, N. Rustogi, I. Riba-Garcia, B. D. Hale, A. M. Phillips, H. Waldvogel, R. Haines, P. Bradbury, A. Stevens, R. L. M. Faull, A. W. Dowsey, G. J. S. Cooper, R. D. Unwin, Commun Biol 2019, 2, 43.

[7] M. Matarin, D. A. Salih, M. Yasvoina, D. M. Cummings, S. Guelfi, W. Liu, M. A. Nahaboo Solim, T. G. Moens, R. M. Paublete, S. S. Ali, M. Perona, R. Desai, K. J. Smith, J. Latcham, M. Fulleylove, J. C. Richardson, J. Hardy, F. A. Edwards, Cell Rep 2015, 10, 633.

[8] N. T. Seyfried, E. B. Dammer, V. Swarup, D. Nandakumar, D. M. Duong, L. Yin, Q. Deng, T. Nguyen, C. M. Hales, T. Wingo, J. Glass, M. Gearing, M. Thambisetty, J. C. Troncoso, D. H. Geschwind, J. J. Lah, A. I. Levey, Cell Syst 2017, 4, 60.

[9] J. Hardy, S. Bayram, M. S. Guelfi, M. Matarin, F. A. Edwards, D. J. A. s. Salih, Dementia, 2018, 14, P1027.

[10] H. Braak, I. Alafuzoff, T. Arzberger, H. Kretzschmar, K. Del Tredici, Acta Neuropathol 2006, 112, 389.

[11] J. Folch, D. Petrov, M. Ettcheto, S. Abad, E. Sanchez-Lopez, M. L. Garcia, J. Olloquequi, C. Beas-Zarate, C. Auladell, A. Camins, Neural Plast 2016.

[12] D. Ferreira, C. Verhagen, J. A. Hernandez-Cabrera, L. Cavallin, C. J. Guo, U. Ekman, J. S. Muehlboeck, A. Simmons, J. Barroso, L. O. Wahlund, E. Westman, Sci Rep 2017, 7, 46263.

[13] H. Huang, S. Nie, M. Cao, C. Marshall, J. Gao, N. Xiao, G. Hu, M. Xiao, Age (Dordr) 2016, 38, 303; J. O. Hollnagel, S. Elzoheiry, K. Gorgas, S. Kins, C. A. Beretta, J. Kirsch, J. Kuhse, O. Kann, E. Kiss, PLoS One 2019, 14, e0209228.

[14] G. Paxinos, K. B. Franklin, *Paxinos and Franklin's the mouse brain in stereotaxic coordinates*, Academic press, 2019.

[15] V. K. Gupta, A. Rajala, R. J. Daly, R. V. Rajala, EMBO Rep 2010, 11, 861; V. Gupta, M. Mirzaei, V. B. Gupta, N. Chitranshi, Y. Dheer, R. Vander Wall, M. Abbasi, Y. You, R. Chung, S.

Graham, Sci Rep 2017, 7, 8412; Y. Dheer, N. Chitranshi, V. Gupta, M. Abbasi, M. Mirzaei, Y. You, R. Chung, S. L. Graham, V. Gupta, Mol Neurobiol 2018, 55, 9043.

[16] L. Deng, K. Pushpitha, C. Joseph, V. Gupta, R. Rajput, N. Chitranshi, Y. Dheer, A. Amirkhani, K. Kamath, D. Pascovici, J. X. Wu, G. H. Salekdeh, P. A. Haynes, S. L. Graham, V. K. Gupta, M. Mirzaei, Front Mol Neurosci 2019, 12, 24; M. Mirzaei, V. K. Gupta, N. Chitranshi, L. Deng, K. Pushpitha, M. Abbasi, J. M. Chick, R. Rajput, Y. Wu, M. J. McKay, G. H. Salekdeh, V. B. Gupta, P. A. Haynes, S. L. Graham, J Cell Biochem 2020.

[17] M. Mirzaei, D. Pascovici, J. X. Wu, J. Chick, Y. Q. Wu, B. Cooke, P. Haynes, M. P. Molloy, Methods Mol Biol 2017, 1549, 45.

[18] A. A. Margolin, S. E. Ong, M. Schenone, R. Gould, S. L. Schreiber, S. A. Carr, T. R. Golub, PLoS One 2009, 4, e7454; K. Kammers, R. N. Cole, C. Tiengwe, I. Ruczinski, EuPA Open Proteom 2015, 7, 11.

[19] K. S. Anand, V. Dhikav, Ann Indian Acad Neurol 2012, 15, 239.

[20] J. Mulder, M. Zilberter, S. J. Pasquare, A. Alpar, G. Schulte, S. G. Ferreira, A. Kofalvi, A. M. Martin-Moreno, E. Keimpema, H. Tanila, M. Watanabe, K. Mackie, T. Hortobagyi, M. L. de Ceballos, T. Harkany, Brain 2011, 134, 1041.

[21] J. Y. Xu, C. Chen, Neuroscientist 2015, 21, 152; A. L. Orr, J. E. Hanson, D. Li, A. Klotz, S. Wright, D. Schenk, P. Seubert, D. V. Madison, Neuron 2014, 82, 1334.

[22] Y. C. Hsieh, C. Guo, H. K. Yalamanchili, M. Abreha, R. Al-Ouran, Y. Li, E. B. Dammer, J. J. Lah, A. I. Levey, D. A. Bennett, P. L. De Jager, N. T. Seyfried, Z. Liu, J. M. Shulman, Cell Rep 2019, 29, 301.

[23] S. Urban, Proc Natl Acad Sci U S A 2016, 113, 1112.

[24] S. S. Adav, J. E. Park, S. K. Sze, Mol Brain 2019, 12, 8.

[25] M. Mirzaei, V. B. Gupta, J. M. Chick, T. M. Greco, Y. Q. Wu, N. Chitranshi, R. Vander Wall, E. Hone, L. T. Deng, Y. Dheer, M. Abbasi, M. Rezaeian, N. Braidy, Y. Y. You, G. H. Salekdeh, P. A. Haynes, M. P. Molloy, R. Martins, I. M. Cristea, S. P. Gygi, S. L. Graham, V. K. Gupta, Sci Rep-Uk 2017, 7.

[26] M. Causevic, U. Farooq, S. Lovestone, R. Killick, Neurosci Lett 2010, 485, 162; S. Gengler, A. Hamilton, C. Holscher, PLoS One 2010, 5, e9764.

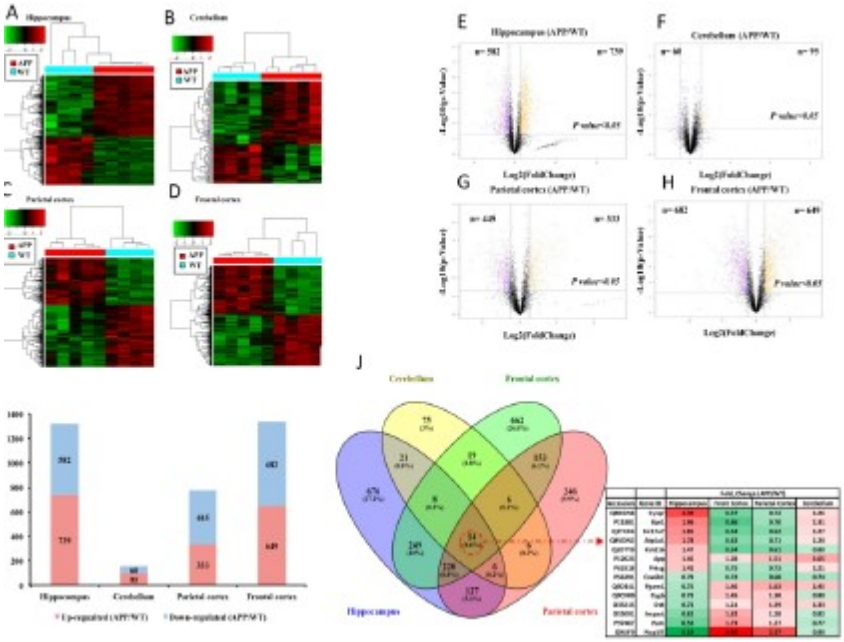

FIGURE 1 Heatmaps (hierarchical clustering) of the log-transformed ratios of differentially expressed proteins from specific brain tissues with AD compared with their corresponding controls. Column colors indicate treatment types (APP/PS1 mice or controls). Red and green color-coding indicate relative increase or decrease in protein abundance, respectively. A. Differentially expressed proteins in hippocampus. B. Differentially expressed proteins in cerebellum. C. Differentially expressed proteins in parietal cortex. D. Differentially expressed proteins in frontal cortex. E-H. Volcano plots demonstrating the dual thresholds for differentially regulated proteins in specific brain sites. Proteins within the upper and outer quadrants meet both the fold change (>1.2 or <0.8333) and pvalue cut-off (<0.05) and are therefore considered as differentially regulated in specific brain areas with AD. E. Regulated proteins in hippocampus. F. Regulated proteins in cerebellum. G. Regulated proteins in parietal cortex. H. Regulated proteins in frontal cortex. I. Bar graph indicating the number of regulated proteins in different brain tissues. J. Venn diagram indicating the overlap among the differentially regulated proteins identified and quantified in four different brain regions. The overlapped 14 regulated proteins in four tissues from APP/PS1 mice brains are listed along with their expression changes. The green and red colors separately represent the down and up regulation in APP/PS1 mice brains

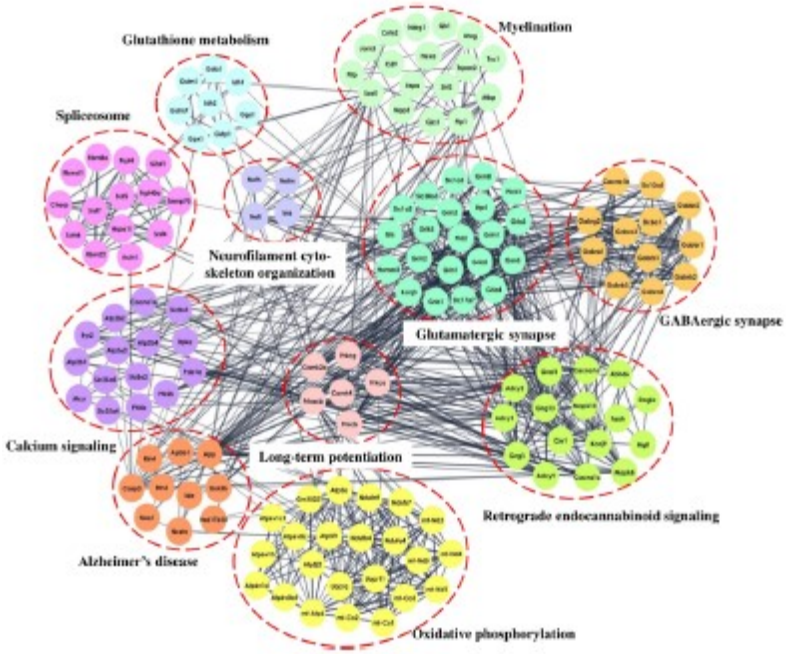

FIGURE 2 Protein networks and associated pathways regulated in AD mice hippocampus region generated by string plugin in Cytoscape. The eleven protein network families including Glutathione metabolism, Spliceosome, Neurofilament cyto-skeleton organization, Glutamatergic synapse, GABAergic synapse, Calcium signaling, Retrograde endocannabinoid signaling, Alzheimer's disease, Long-term potentiation, Myelination and oxidative phosphorylation were identified

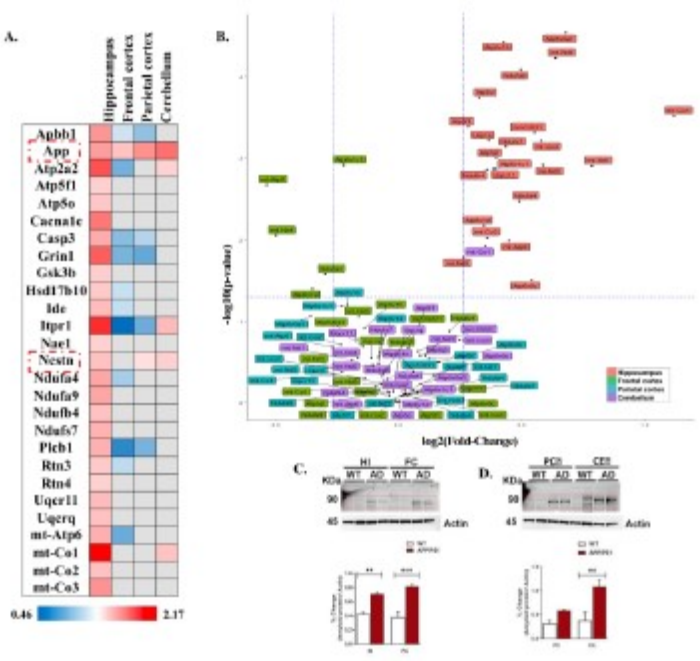

FIGURE 3 A. proteins involved in Alzheimer's disease pathway and their expression pattern in four different brain sites. B. Scatter plots generated with regulated proteins in oxidative phosphorylation pathway and their expression changes in four different brain sites. Four different colors indicate specific brain areas. Horizontal and vertical lines are the cut off of p-value and fold changes, respectively. Proteins in the top left and right corners are down- and up-regulated respectively. C-D. Western blots of younger brain lysates from HI, FC, PC, CE from WT and APP/PS1 mice were probed with Amyloid β (90 KDa) and used Actin as a loading control